The Offshore Chlorophyll Maximum in S. Lake Michigan: Chlorophyll Distribution in Relation to Sediment Concentrations and the Thermal Bar

Katherine M Strojny[1], Scott F. Diehl[2], Haibo Wan[2], and Judith W. Budd[2]

Department of Biological Sciences, Michigan Technological University, Houghton, MI 49931

Department of Geological Engineering and Sciences, MTU [2]

ABSTRACT

Time series SeaWiFS (Sea-viewing Wide Field-of-View Sensor) imagery revealed significant productivity pulses (elevated Chl a) associated with resuspended sediments in Lake Michigan over an eight month period from September to the end of April. Analysis of simultaneously collected SeaWiFS (Sea-viewing Wide Field-of-view sensor) sediment and chlorophyll maps and AVHRR (Advanced Very High Resolution Radiometer) lake surface temperature imagery revealed distinct horizontal physical and biological gradients from nearshore to offshore in late March and April in Lake Michigan. The thermal bar (4 degree C water of highest density) constituted a transition zone from nearshore (warmer) to offshore (colder) waters. We identified two chlorophyll maxima in nearshore and offshore waters, which were separated by the thermal bar in SeaWiFS chlorophyll and PSS data of southern Lake Michigan in late spring. Whereas the nearshore chlorophyll maxima was strongly coupled to resuspended sediment, the offshore chlorophyll maxima was not. Such "out of season" responses were previously nearly impossible to document, given unpredictable and hazardous working conditions at that time of year.

The combination of PSS data and SeaWiFS imagery demonstrate the similarity between vertical and horizontal spatial patterns during resuspension events. The vertical distribution of chlorophyll and location of the offshore thermal bar coincide with the horizontal distribution of chlorophyll (as C_{SAT}) and the location of the thermal bar (as seen in satellite-derived lake surface temperature (LST) images). The PSS data show a nearshore and offshore chlorophyll maxima separated by a region of low chlorophyll concentration. At times when the thermal bar is present, the PSS chlorophyll minimum is located at or near the thermal bar. Combined SeaWiFS C_{SAT} and AVHRR LST images show the exact same patter. This offshore productivity maxima could have significant implications for lower trophic food web interactions, by alleviating starvation and energizing the base of food webs at the very time when resources are most scarce (e.g., mid-winter, unstratified period).

We calculated the total mass of sediment of the plume per day. The process involved calculation of the mass of sediment at each pixel, which was then summed for all of the pixels in each region for each of the validations. A total mass for each day was obtained by summing the nearshore and offshore masses. The results ranged from 0.2 kg x 10^9 to a high of 2.6 kg x 10^9 on March 26 and 0.25 to 1.0 kg x 10^9 for 1998 and 1999, respectively. A similar technique will be used to calculate the mass of nearshore versus offshore chlorophyll in future studies using Great Lakes SeaWiFS

EEGLE STUDY SITE

LAKE MICHIGAN

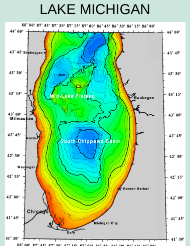

- o Lake Michigan is the sixth largest lake in the world.
- o Its hydraulic residence time is 62 years (Quinn 1992), however for particle-reactive constituents, internal removal through sedimentation is much more rapid.
- o The distribution of post-glacial sediment in southern Lake Michigan is asymmetric with the greatest accumulations found within 20 km from the eastern shore and decreasing towards the deepest sounding in the basin.

Quinn, F.H. 1992. Hydraulic residence times for the Laurentian Great Lakes. *J. Great Lakes Res.* 18:22-28.

EEGLE REMOTE SENSING STUDIES

HYPOTHESES

Episodic Nature: How dramatic are southern Lake Michigan resuspension events and how much do they depart from ten year average conditions? Quantifying the historical magnitude of turbidity plumes provides valuable information for numerous historical comparisons.

Dependency Hypothesis: Several contingencies influence turbidity plume development and cross margin transport. How important are ice pack surges and ice scour along the shoreline in mediating cross margin transport? What is the relationship of thermal bar formation to coastal plume development in the southern basin? How do other coastal phenomena (e.g., impact of river plumes) influence cross margin transport on a seasonal and interannual basis?

METHODS

SeaWiFS and AVHRR Image Processing

o Satellite imagery, which are received from the NASA Goddard Distributed Active Archive Center (DAAC) and the NOAA Satellite Active Archive (SAA), are processed in near real-time for AVHRR and after a two week delay for SeaWiFS.

o Routine processing of SeaWiFS imagery is accomplished using a near coastal atmospheric correction procedure with automated image processing methods based on the NASA IDL/SeaDAS code. The SeaWifS standard atmospheric correction routine produces negative radiances and overestimates chlorophyll in the Great Lakes. The modified correction developed for coastal waters (see Stumpf et al. 1998) removes negative radiances and provides more stable and valid results for chlorophyll.

o SeaWiFS is sensitive to the wavelengths at 410, 440, 490, 510, 555, 670, 760, and 860 nm. The first six visible channels provide remote sensing reflectance (RRS) and the two near infrared channels (760 and 860 nm) are used to remove atmospheric contamination. The ratio of the RSR at 490 and 555 can be used to estimate chlorophyll, while RSR at 555 or 670 is used to estimate seston.

Stumpf, R.P. and others. 1998. Ocean Color Algorithms for Remote Sensing Coastal Waters of the U.S. Southeast and Easter Gulf of Mexico. EOS, Transactions, American Geophysical Union, 13:1559-1569.

Table 1: **Sensor Characteristics of the AVHRR and SeaWiFS instruments**.

Satellite Sensor	Limnologic Phenomena	Channel	Wavelength (ug)	Spatial Resolution (km^2)	Temporal Resolution
AVHRR	Reflected solar energy; suspended sediment, coastlines, and clouds	1	0.58-0.68 (red)	1.1 km^2	4-6/day
	Reflected solar energy; coastlines, and clouds	2	0.72-1.00 (near-IR)	1.1 km^2	4-6/day
	Reflected solar energy; thermal emission; clouds and sea surface temperature	3	3.55-3.93 (mid-IR)	1.1 km^2	6-10/day
	Thermal emission; clouds and sea surface temperature	4	10.3-11.3 (thermal IR)	1.1 km^2	6-10/day
	Thermal emission; clouds and sea surface temperature	5	11.5-12.5 (thermal IR)	1.1 km^2	6-10/day
SeaWiFS	Reflected solar energy; gelbstoffe	1	0.412 (violet)	1.0 km^2	1/day
	Reflected solar energy; chlorophyll absorption	2	0.443 (blue)	1.0 km^2	1/day
	Reflected solar energy; pigment absorption	3	0.490 (blue-green)	1.0 km^2	1/day
	Reflected solar energy; chlorophyll absorption	4	0.510 (blue-green)	1.0 km^2	1/day
	Reflected solar energy; pigments, optical properties, sediments	5	0.555 (green)	1.0 km^2	1/day
	Reflected solar energy; atmospheric correction (CZCS heritage)	6	0.670 (red)	1.0 km^2	1/day
	Reflected solar energy; atmospheric correction, aerosol radiance	7	0.765 (near-IR)	1.0 km^2	1/day
	Reflected solar energy; atmospheric correction, aerosol radiance	8	0.865 (near IR)	1.0 km^2	1/day

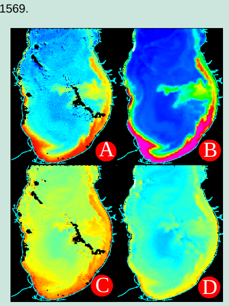

Fig 1. Example of SeaWiFS RSR (top) and Chlorophyll (bottom) maps showing missing pixels associated with cloud contamination on March 22, 1998 (A & C) and the interpolated product (B & D).

Cloud Removal Using Time-Space Interpolation

Clouds are a major impediment to the visualization of coastal processes from satellite instruments. In this investigation, we used a statistically-based objective interpolation technique to estimate cloud contaminated pixels. Chlorophyll interpolation is possible because there is a relationship between chlorophyll and its neighbors in both space and time. The objective interpolation technique, which has been used successfully in a variety of studies (e.g., Bretherton et al. 1976, Carter and Robinson 1987, Mariano and Brown 1992, Ransibrahmanakul 1996) is based on the Gauss-Markoff theorem (Liebelt 1967). This method, which is recommended because of its simplicity and robustness, provides chlorophyll and turbidity optimal estimates for cloud-contaminated pixels (see third panel of poster for results).

References

Bretherton, F.P., R.E. Davis, and C.B. Fandry. 1976. A technique for objective analysis and design of oceanographic experiments applied to MODE-73. Deep-Sea Research 23: 559-582.

Gordon, H.R. and A.Y. Morel. 1983. Remote assessment of ocean color for interpretation of satellite visible imagery: review. Lecture Notes on Coastal and Estuarine Studies, 4, Springer-Verlag, 114 pp.

Inoue, H. 1986. A least-squares smooth fitting for irregularly spaced data: Finite-element approach using the cubing B-spline basis. Geophysics 51: 2051-2066.

Liebelt, P.B. 1967. An Introduction to Optimal Estimation. Addison-Wesley Publishing Company, Reading, Massachusetts.

Mariano, A.J., and O.B. Brown. 1992. Efficient objective analysis of dynamically heterogeneous and nonstationary fields via the parameter matrix. Deep-Sea Research 39: 1255-1271.

Ransibrahmanakul, V. 1996. Variability of Eddy Heat Fluxes Over the Northwestern Gulf of Mexico. A Ph.D. dissertation, Louisiana State University, Baton Rouge.

ACKNOWLEDGMENTS

This research is supported under the auspices of the KITES (Keweenaw Interdisciplinary Transport Experiment in Superior) and EEGLE (Episodic Events-Great Lakes Experiment) projects, which are funded by the National Science Foundation and the National Oceanic and Atmospheric Administration.

Frequency of Events

Recent satellite tracking of southern Lake Michigan coastal plumes over an eight year period from 1992 to 1999, as well as water intake records from St. Joseph, Michigan and Chicago, Illinois (from Eadie, EEGLE webpages online resource), reveal surprising high frequency of resuspension events, although the areal extent (seen in satellite imagery) and relative magnitude in terms of mass of resuspended sediment varies greatly from event to event.

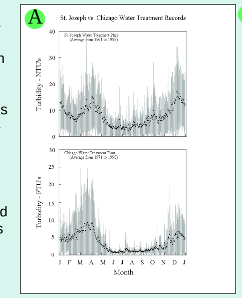

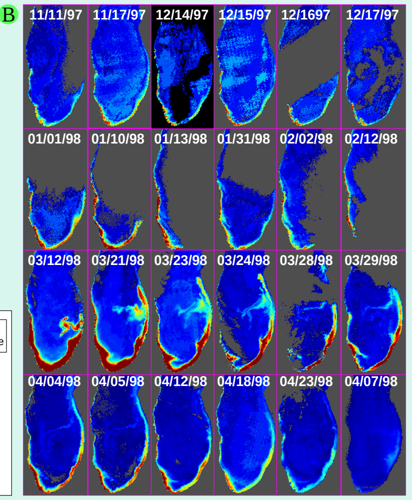

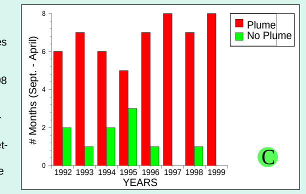

Fig. 2 (A) St. Joseph and Chicago water treatment records show great seasonality in the magnitude of events, with highest turbidity at intakes during November through May. (B) AVHRR images of the eight month period from October 1997 to May 1998 shows the areal extent and relative magnitude of coastal resuspension events in southern Lake Michigan for one year. (C) A count of cloud free satellite images provides a rough metric of how often resuspended sediments can be detected in the satellite imagery

S. LAKE MICHIGAN PLUME TIME SERIES

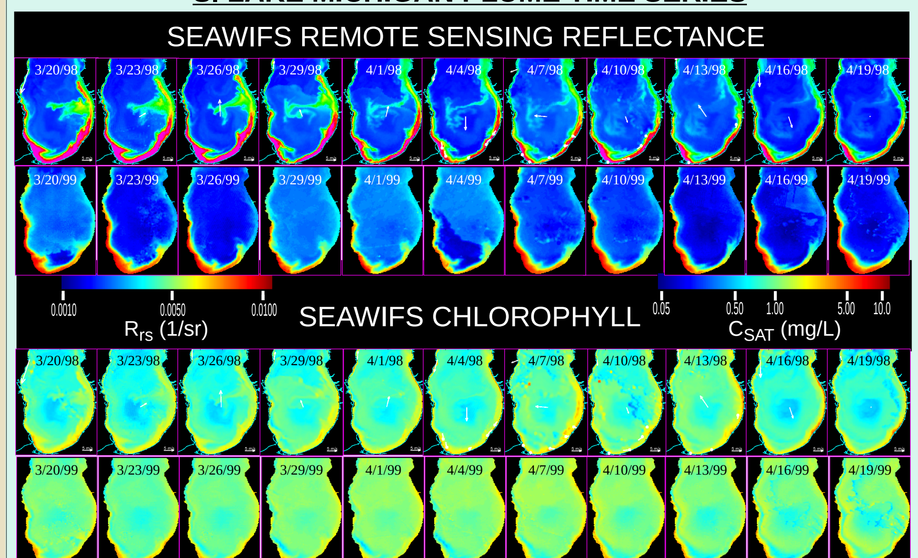

1998 TIME SERIES: The 35-day time series from March 19 to April 22 provides striking details of surface sediment and chlorophyll concentrations in southern Lake Michigan. The plume, which originated near Port Washington, Wisconsin can be tracked along the southern shoreline over 500 km to Ludington, Michigan. Several offshore features are also evident in the imagery originating at Chicago, Illinois, St. Joseph and Muskegon, Michigan. The most pronounced example of cross margin transport was a coastal "squirt" near Muskegon, which extended offshore into the center of the lake, a distance of 75 km. This feature contorted over the next three weeks and finally dissipated in the southwestern basin around 4/11/99. Chlorophyll concentrations were clearly enhanced along the plume track consistent with field sampling results indicating high phosphorus concentrations in the plume. An intriguing "donut" shaped feature appeared just outside the plume track in late March and persisted for three weeks, indicating a productive offshore zone; however, we found no evidence of enhanced sediment concentrations at the same locations. Both the RSR and chlorophyll images indicate uniformly low concentrations of materials in the central southern basin for the entire period.

1999 TIME SERIES: This series encompassed a slightly longer period from March 6th through May 3rd, 1999. In this series, the areal extent of the plume is somewhat truncated as compared with 1998, particularly in the eastern basin north of Grand Haven. There were two small plumes that developed and moved in a counter-clockwise direction at Chicago and Grand Haven, Michigan. In late March/early April the plumes still exist, but their areal extent is greatly diminished. By late April/early May, the plume is constrained to the southern-most tip of Lake Michigan. We observed two distinct maxima and two distinct minima in chlorophyll production, identical to 1998. The maxima occurred along the coast coincident with the sediment plume and then again offshore in the shape of a donut. The central minima is surrounded by the toroidal (donut) shaped off-shore maxima. A second crescent-shaped minima located in the southern basin separates the off-shore maxima from the near-shore maxima. A thread of the crescent-shaped offshore minima continues up the western coast and to a lesser extent along the east coast.

Offshore Chlorophyll Maximum

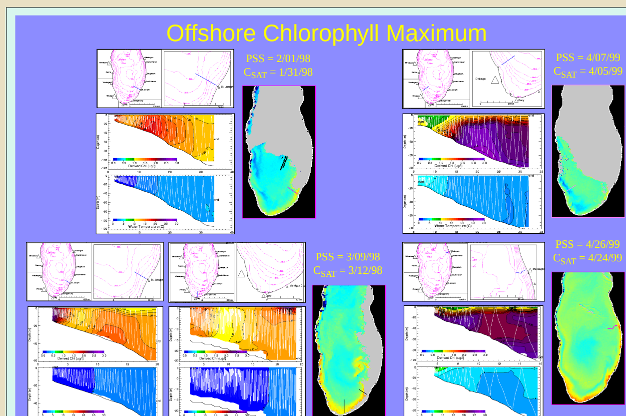

Comparison of PSS and Satellite Data

PSS data are used to demonstrate the similarity between vertical and horizontal spatial patterns during resuspension events. The vertical distribution of chlorophyll and location of the offshore thermal bar coincide with the horizontal distribution of chlorophyll (as C_{SAT}) and the location of the thermal bar (as seen in satellite-derived lake surface temperature (LST) images). The PSS data show a nearshore and offshore chlorophyll maxima separated by a region of low chlorophyll concentration. At times when the thermal bar is present, the minima is located at or near the thermal bar. This intriguing offshore productivity maxima, which is described here for the first time, could have very significant implications for lower trophic food web interactions, by alleviating starvation and energizing the base of food webs at the very time when resources are most scarce (e.g., mid-winter, unstratified period). The fundamental consequences are reduction of competition when resources are at their minimum, maintaining over-wintering taxa and promoting diversity.

THERMAL FRONT DETECTION

Distinct biological and chemical gradients often exist between highly productive nearshore and less productive offshore zones of lakes. Physical processes, such as the seasonally recurring thermal bar (a vertical shore parallel density maxima at 4 ^{o}C) and wind-driven circulation, may inhibit the transport of materials from nearshore lake margins to offshore regions. Here we demonstrate the results of an edge detection algorithm, which through successive statistical iterations, maps thermal fronts, such as the 4 ^{o}C isotherm, within southern Lake Michigan. These images are the result of merging lake surface temperature fronts maps with turbidity and chlorophyll maps.

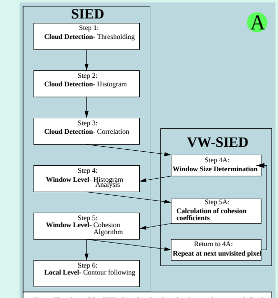

Fig 1. Flowchart of the SIED algorithm detailing the changes that are made for the VW-SIED algorithm.

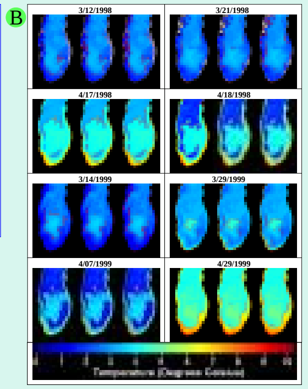

Fig 4. (A) We investigated the effects of using a geographic window size with an existing edge detection technique. A geographic window is one whose size is not constant, but is determined by the correlation of the data surrounding the window's central point. Using this approach instead of a fixed window size, the investigation window is optimized for all of the image, providing more reliable detection of edges within the window. (B) The new algorithm was run on several SST images from S. Lake Michigan and compared to runs of the original algorithm and a modification of the original algorithm optimized for this region. The results show that the geographic window improves edge detection most in the near-shore regions, and to a lesser extent in the off-shore regions.

DATA FUSION

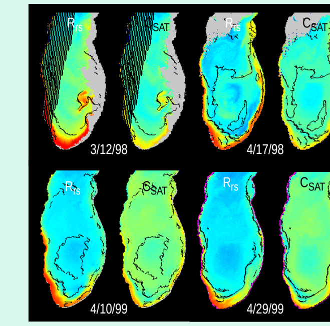

Fig. 5. Example of data fusion product from VW-SIED and SeaWiFS R_{rs} and C_{SAT} imagery. Thermal fronts shown in the April images indicate the location of the 4oC thermal bar. The late spring CSAT images for 1998 and 1999 show the presence of two chlorophyll maxima-- a nearshore maximum that is coupled with the sediment plume and an offshore "donut"-shaped maximum-separated by the thermal bar. Simultaneously acquired AVHRR LST front imagery and SeaWiFS R_{rs} and C_{SAT} maps indicate that the thermal fronts are generally lakeward of the nearshore sediment and chlorophyll fronts. Note that the offshore chlorophyll maxima, which is offshore of the thermal front, is not coupled with sediment.

MASS CALCULATION

METHODS

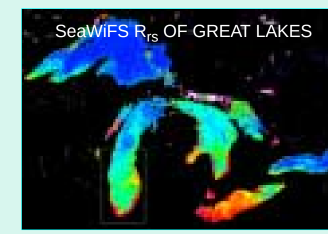

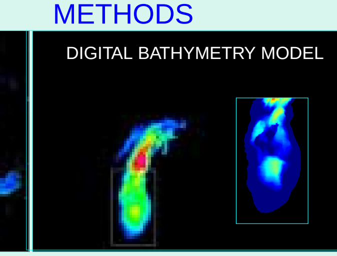

STEP 1.

Using Arc/Info, raster bathymetry of Lake Michigan was projected and co-registered with the standard georeferenced SeaWiFS imagery for the Great Lakes. The image processing package, PCI EASI, was used to create a subset of the bathymetry corresponding to the EEGLE study area in S. Lake Michigan (SLM).

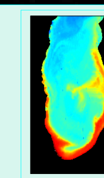

STEP 2.

An interpolated time series was created using OA on SeaWiFS R_{rs} imagery obtained during the study period. The result was a series of daily images showing R_{rs}, standardized at 1800 EST, with temporal gaps where cloud cover prevented a quality interpolation product.

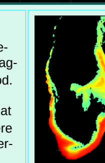

STEP 3.

For each interpolated image in the time series, low-R_{rs} areas were masked so that the calculation could be performed only on the nearshore and offshore plume features. The images were thresholded to eliminate most of the offshore (low sediment) pixels, such that a nearly-contiguous nearshore plume was identified.

STEP 4.

Mass calculations were based on retrievals from the near and offshore sediment plume. Plume pixels were divided into nearshore and offshore regions based on bathymetric depth. A nearshore depth of 40 m captured most of the March 1998 nearshore plume event. Sediment concentrations in the nearshore (depth < 40m) were assumed to be well-mixed and therefore constant throughout the water column; whereas offshore plume features were considered a surface feature with constant mixing to a fixed depth, 40 m, below which TSS concentrations were assumed to drop off.

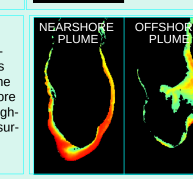

STEP 5.

For each pixel, the SeaWiFS digital number (DN) for R_{rs} was converted to R_{rs} (steradians^{-1} or sr^{-1}) and percent reflectance (R_{rs}%) using:

$$\mathbf{DN = [(\log10 (R_{rs}) + A)\, B] + 0.5}$$

where coefficients A = 4 and B = 85 for SeaWiFS channel 5 (R_{rs}). R_{rs} (sr^{-1}) was expressed as R_{rs}% using the relation $\%R_{rs} = 100\,\pi\, R_{rs}$.

STEP 6.

Using the validation equations shown in Table 1, TSS concentrations were then calculated at each pixel using R_{rs} from the interpolated time series.

Table 1: R_{rs} TSS Validations

Source	Description	Equation
Ji Rubao et al. (in review)	1998 SLM plume only	TSS = 1.0888 $e^{84.739\ Rrs}$ (Rrs expressed as fraction of 1)
Warrington (IAGLR 2000)	1998 SLM	$\%R_{rs}$ = 0.60 TSS + 1.30
Budd et al. (in prep.)	Average 1998/1998 SLM	$\%R_{rs}$ = 1.05 TSS + 0.75

RESULTS

Using the nearshore and offshore mixing assumptions (constant concentration and constant concentration from 0 to 40 m depth, respectively), we calculated the total mass of sediment of the plume per day. The process involved calculation of the mass of sediment at each pixel, which was then summed for all of the pixels in each region for each of the validations. A total mass for each day was obtained by summing the nearshore and offshore masses.

The results using the Ji et al. (in review) validation equation are presented in Fig. 6 below for the 1998 and 1999 spring resuspension event. The mass of sediment in March1998 was estimated to be ~2.0 kg x 10^9 to a high of 2.6 kg x 10^9 on March 26. Estimated masses at the end of the event in mid-April ranged from 0.5 to 1.0 kg x 10^9. The 1999 estimates of daily mass were considerably lower in the range of 0.25 to a high of 1.0 kg x 10^9 in early March. These observations are consistent with the observed spatial extent of the plumes in 1998 and 1999.

Ji, R., C. Chen, D.J. Schwab, D. Beletsky, J.W. Budd, G.L. Fahnenstiel, T.H. Johengen, H. Vanderploeg, B.J. Eadie, M. Bundy, In prep. "Influence of Suspended sediments on the ecosystem in Lake Michigan: A 3-D coupled bio-physical modeling experiment.

Fig 6. SLM1998/1999 Total Daily Sediment Mass

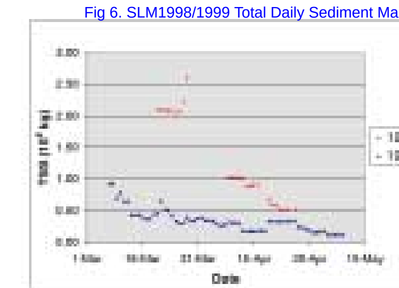

NEXT STEPS

Validate and improve: Perform validations including comparing with results of other models. Potential improvements may include modifying the vertical concentration assumptions and tuning the interpolation process to reduce or remove temporal gaps.
Repeat: Perform sediment mass calculation for spring 2000 and other resuspension events.
Extend: Apply the concept of using interpolated C_{SAT} time series to calculation of daily chlorophyll concentrations in southern Lake Michigan.